Department of
Information Engineering
and Computer Science
DISI

UNIVERSITY
OF TRENTO - Italy

DISI - Via Sommarive, 9 - 38123 POVO, Trento - Italy
http://disi.unitn.it

A Joint Network/Control Design for Cooperative Automatic Driving: Extended Version

Giulia Giordano, Michele Segata,
Franco Blanchini, Renato Lo Cigno

August 2017

Technical Report # DISI-17-012

Abstract

Cooperative automatic driving, or platooning, is a promising solution to improve traffic safety, while reducing congestion and pollution. The design of a control system for this application is a challenging, multi-disciplinary problem, as cooperation between vehicles is obtained through wireless communication. So far, control and network issues of platooning have been investigated separately. In this work we design a cooperative driving system from a joint network and control perspective, determining worst-case upper bounds on the safety distance subject to network losses, so the actual inter-vehicle gap can be tuned depending on vehicle or network performance. By means of simulation, we show that the system is very robust to packet losses and that the derived bounds are never violated.

1 Introduction

Traffic congestion and safety are still two major problems of modern transportation on roads. One promising solution to such problems is cooperative driving. By means of wireless communication, vehicles share information about their status and the sensed surrounding environment, which drastically increases the perception of what happens around them, enabling cooperation. Using only standard in-car sensors, as currently done by prototype self-driving vehicles, does not empower this ability, thus in many ways self-driving vehicles share the same limitations of human drivers. As an example, a wireless link can let a vehicle know the *future* intended trajectory of another one (at an intersection, as a long term destination or cruising speed, etc), a feat that no on-board sensor can do.

To reduce highway congestion, the community has proposed an application called Cooperative Adaptive Cruise Control (CACC): a communication-enhanced version of a standard Adaptive Cruise Control (ACC) that is capable of maintaining a very small inter-vehicle spacing while ensuring passengers' safety. The CACC forms trains of vehicles, called *platoons*, so this application is also known with the name of *cooperative automatic driving*, or *platooning*. Platooning provides benefits in terms of efficiency, safety, and driving comfort [1, 2]. Lowering the inter-vehicle gap results in a better use of the road infrastructure (where most of the space is now simply wasted due to safety distances), improves traffic flow and thus reduces congestion and, at the same

time, the waste of fuel due to start and stop dynamics caused by congestion itself. Safety is improved because an automated systems takes control over human driving, which, as shown by statistics, is the cause of more than 90 % of the accidents [3]. Finally, comfort is improved as there is no longer the need to focus on driving, so the "former driver" is free to do other activities.

The design of a cooperative driving system is a control-theoretical problem that is inevitably intertwined with networking problems. The input to the control algorithm is information about the other vehicles in the platoon, such as speed, position, or acceleration, which is conveyed via wireless links, through periodic broadcast (or beaconing), as well as via local sensors that can improve the precision of distance and relative speed measures. Given the inherent nature of a wireless link, data packets can be lost, which in turn has a dramatic impact on the performance of the application. Bad performance of autonomous driving can result in injuries or loss of life.

Most of the works in the field do not consider, or consider only partially, the impact of wireless impairments on the performance of the control system. In this paper we design a cooperative driving algorithm that specifically takes into account error dynamics due to loss of data and ensures that a predefined safety bound is never violated, given a particular worst-case scenario. To the best of our knowledge, this is the first attempt to jointly design a control algorithm and a dedicated communication protocol that takes into account packet losses. The main features of our proposal can be summarized as follows:

- The design jointly considers control and network performance. The controller parameters can be tuned to obey some predefined bounds on the position error, given an upper bound on the input error caused by network impairments (Sections 3 and 4). By means of simulations, we show that the controller never violates the imposed safety constraints (Section 5);

- The algorithm is capable to maintain a constant spacing policy thanks to a leader plus bidirectional control topology, which comes with no additional network overhead with respect to a commonly assumed leader-plus predecessor-following scheme (see Sections 2 and 5);

- The vehicles in the platoon share a common target speed, which can be changed by an external authority, e.g., an optimal speed advisory infrastructure.

2 Background and Related Work

The design of a cooperative automatic driving (or platooning) system is definitely a challenging task, as is witnessed by the large body literature on the topic. Different solutions have been proposed, with different design assumptions and thus characteristics. The main goal is to keep the inter-vehicle gap as small as possible, while ensuring passengers' safety. The key difference to standard ACC solutions is the use of wireless communication for sharing control data with potentially all the vehicles in the platoon. Wireless communication allows a vehicle to "see" behind other vehicles, which is not possible by using standard radar sensors. In addition, by means of communication, a vehicle can inform the others about what it is going to do, letting them "know the future".

A key design choice is the *logical control topology*, indicating from which members each vehicle is considering data to compute the control action. This is different from the actual network topology, which is typically broadcast-like. Even if the network topology is a full mesh, the control algorithm may simply exploit a subset of the received information. As an example, the controllers in [4–6] implement a predecessor-following topology, where each vehicle is using the information of its predecessor only. Other examples include a leader- and predecessor-following topology [7, 8], which considers in addition the information of the first vehicle. We also find bi-directional [9] and potentially all-to-all [10] control topologies.

The choice of the control topology has implications on the system performance, in particular with respect to the gap policy. Predecessor-following control topologies are proven to be string-stable only under a constant time headway gap policy [4, 7]. This means that the distance is constant in time, so the faster the vehicles, the larger the gap. If this policy is not respected, then the string-stability property is violated, so distance errors at the head of the platoon might be propagated and amplified towards the end, potentially leading to collisions. By adding a link to the leader, instead, the system can be string-stabilized with respect to a constant spacing gap, i.e., the distance is fixed and it is not related to cruising speed [7].

String-stability, however, is not generally related to the distance (or the time headway) vehicles should maintain to avoid collisions in case of packet losses. The performance of a cooperative automatic driving system is typically analyzed with a pure control-theoretic approach, so that a quantitative characterization of the safety gap as a function of the network conditions is

hard to find in the literature [11].

Due to this missing link between the control and the networking communities, we find studies that try to understand the impact of network impairments a posteriori [12]. In addition, we find several studies working from the network perspective, trying to improve the efficiency of the protocol and thus maximizing the packet delivery probability.

An example is the work in [13]. The work exploits the intrinsic structure of the platoon and combines intra-platoon synchronization with transmit power control, reducing random channel contention and interference to farther vehicles. Similarly, the work in [14] focuses on synchronization, both from the communication and from the actuation point of view, showing benefits and downsides of five different approaches. Other works trying to coordinate channel access to reduce contention can be found in [15–18]. Some of these approaches implement a reliable delivery scheme, which detects lost packets and attempts retransmission, thus recovering lost information.

The work in [19] brings together these ideas (i.e., coordination, transmit power control, and reliable delivery) with an additional point: a dynamic message dissemination rate. The idea is to reduce the amount of data injected in the network by sending packets only when really needed. The message dissemination rate is changed depending on the jerk, i.e., on how much the acceleration of the vehicle has changed with respect to the last sent packet. Missing information is computed by other vehicles through interpolation.

Clearly, all the works focusing only on a single communication technology do not provide solutions to a complete network black out. In such a case, the system can fallback to a purely sensor-based system [20] or rely on a backup communication technology. As an example, modern LED lamps can be exploited to realize Visible Light Communication (VLC), creating a direct vehicle-to-vehicle communication channel which perfectly suits platooning requirements [21–25].

Another potential alternative is a cellular link [26]. 4G and 5G cellular technology are starting to offer functionalities for direct car-to-car communication, which could also serve as a backup link. Whether this can really be used for the purposes of platooning and what the implications for the cellular network will be are still open issues.

In this work we address communication problems for platooning in a multi-disciplinary way. We present a joint network and control design of a cooperative automatic driving system. Our work derives a theoretic bound on the minimum inter-vehicle distance subject to packet losses is derived in a

Table 1: Main notation used in the paper.

y_i	position of vehicle i
$v(t)$	reference speed
d	desired distance between vehicles
k	elastic coefficient
h	inter-vehicle friction coefficient
r	vehicle-reference friction coefficient
δ_i	communication-induced disturbance term
N_L	maximum number of consecutive packets lost
T	Beacon interval

worst-case scenario. If the conditions considered for the worst-case analysis never occur, then the inter-vehicle distance can never be smaller than the computed bound. To the best of our knowledge, this is the first attempt to realize such kind of control system.

3 Control Algorithm

The goal of our control model is to empower good cooperative driving performance and, at the same time, provide an analytic framework for the design of the communication system in terms of information loss. We propose a class of distributed controllers (which can be seen either as spring-damper mechanical systems, or as impedance-matched electromagnetic systems, [27]) that ensure string stability as proven by Eq. (23) in Section 3.3.

The control action depends on information about the vehicle in front and the one behind (predecessor-follower topology), and all vehicles are "glued" together by a common dynamic reference speed $v(t)$, which can be imposed by the first vehicle of the platoon, thus having a control topology similar to [7], or can be decided by any other vehicle or taken from an external source (e.g, speed indications coming from the infrastructure). Even the leader follows the reference speed with a transient. Table 1 reports the main notation used throughout the paper.

We consider the following dynamic model: for vehicle 1 (the leader),

$$\ddot{y}_1 = -k(y_1 - y_2 - d) - h(\dot{y}_1 - \dot{y}_2) - r(\dot{y}_1 - v) + \delta_1, \tag{1}$$

for vehicles $i = 2, \ldots N-1$,

$$\begin{aligned} \ddot{y}_i = &-k(y_i - y_{i+1} - d) - k(y_i - y_{i-1} + d) \\ &- h(\dot{y}_i - \dot{y}_{i+1}) - h(\dot{y}_i - \dot{y}_{i-1}) - r(\dot{y}_i - v) + \delta_i \end{aligned} \tag{2}$$

and, for vehicle N,

$$\ddot{y}_N = -k(y_N - y_{N-1} + d) - h(\dot{y}_N - \dot{y}_{N-1}) - r(\dot{y}_N - v) + \delta_N, \tag{3}$$

where, besides the control algorithm coefficients h, k, and r, δ_i is a disturbance factor essentially due to packet losses. Indeed, packet losses are the dominant source of disturbance, as discussed in Section 4.

3.1 Analysis

To simplify the analysis, we consider the model in Eqs. (1) to (3) with $d = 0$. This is equivalent to changing the variables as

$$\hat{y}_i = y_i + d(1 - i), \quad i = 1, \ldots, N,$$

so that the condition $\hat{y}_1 = \hat{y}_2 = \cdots = \hat{y}_N$ is achieved when the true distance between consecutive vehicles is d as desired; we drop the hat to keep the notation simpler.

Let $\bar{\mathbf{1}}$ be the all-one vector

$$\bar{\mathbf{1}}^\top = [\ 1\ 1\ \ldots\ 1\ ]$$

and define the average position as

$$a(t) = \frac{\sum_{i=1}^{N} y_i}{N} = \frac{\bar{\mathbf{1}}^\top y}{N}.$$

Then we introduce a new vector $z(t)$ whose components are the differences $z_i = y_{i-1} - y_i$, $i = 2, \ldots, N$:

$$\begin{bmatrix} z_2(t) \\ z_3(t) \\ \vdots \\ z_N(t) \end{bmatrix} = \begin{bmatrix} 1 & -1 & 0 & \ldots & 0 & 0 \\ 0 & 1 & -1 & \ldots & 0 & 0 \\ \vdots & \vdots & \vdots & \ddots & \vdots & \vdots \\ 0 & 0 & 0 & \ldots & 1 & -1 \end{bmatrix} \begin{bmatrix} y_1(t) \\ y_2(t) \\ y_3(t) \\ \vdots \\ y_N(t) \end{bmatrix}, \tag{4}$$

which can be synthetically written as

$$z(t) = Dy(t),$$

where $D \in \mathbb{R}^{(N-1)\times N}$ is the matrix appearing in Eq. (4). Note that the compound vector $[\ a(t)\ \ z^\top(t)\ ]^\top$, including the average and the differences, is in one-to-one correspondence with $y(t)$.

Let us now define the Laplacian matrix $L \in \mathbb{R}^{N\times N}$ as

$$L \doteq D^\top D = \begin{bmatrix} 1 & -1 & 0 & 0 & \dots & 0 & 0 & 0 \\ -1 & 2 & -1 & 0 & \dots & 0 & 0 & 0 \\ 0 & -1 & 2 & 1 & \dots & 0 & 0 & 0 \\ \vdots & \vdots & \vdots & \vdots & \ddots & \vdots & \vdots & \vdots \\ 0 & 0 & 0 & 0 & \dots & -1 & 2 & -1 \\ 0 & 0 & 0 & 0 & \dots & 0 & -1 & 1 \end{bmatrix}$$

and matrix $M \in \mathbb{R}^{(N-1)\times(N-1)}$ as

$$M \doteq DD^\top = \begin{bmatrix} 2 & -1 & 0 & 0 & \dots & 0 & 0 & 0 \\ -1 & 2 & -1 & 0 & \dots & 0 & 0 & 0 \\ 0 & -1 & 2 & -1 & \dots & 0 & 0 & 0 \\ \vdots & \vdots & \vdots & \vdots & \ddots & \vdots & \vdots & \vdots \\ 0 & 0 & 0 & 0 & \dots & -1 & 2 & -1 \\ 0 & 0 & 0 & 0 & \dots & 0 & -1 & 2 \end{bmatrix}.$$

As can be immediately verified, the following identities hold:

$$D\bar{\mathbf{1}} = 0, \tag{5}$$

$$L\bar{\mathbf{1}} = 0. \tag{6}$$

Consider the Singular Value Decomposition of matrix D:

$$D = P[\ \bar{\mathbf{0}}_{\mathbf{N-1}}\ \Omega\ ]Q^\top, \tag{7}$$

where $\bar{\mathbf{0}}_{\mathbf{N-1}}$ is an all-zero vector of size $N-1$, matrix $\Omega \in \mathbb{R}^{(N-1)\times(N-1)}$ is diagonal and its positive diagonal entries are the singular values of D, while $P \in \mathbb{R}^{(N-1)\times(N-1)}$ and $Q \in \mathbb{R}^{N\times N}$ are orthonormal matrices, hence

$P^\top P = I_{N-1}$ and $Q^\top Q = I_N$ (where I_k denotes the identity matrix of size k). Then we can express the Laplacian matrix as

$$\begin{aligned} L = D^\top D &= Q[\ \bar{\mathbf{0}}_{\mathbf{N-1}}\ \Omega\ ]^\top[\ \bar{\mathbf{0}}_{\mathbf{N-1}}\ \Omega\ ]Q^\top \\ &= Q \begin{bmatrix} 0 & \bar{\mathbf{0}}_{\mathbf{N-1}}^\top \\ \bar{\mathbf{0}}_{\mathbf{N-1}} & \Omega^2 \end{bmatrix} Q^\top \doteq Q\Lambda^2 Q^\top, \end{aligned} \tag{8}$$

where $\Lambda^2 \in \mathbb{R}^{N\times N}$ is a diagonal matrix whose diagonal entries are the eigenvalues of the Laplacian matrix L, given by 0 and the diagonal entries of Ω^2. Since it will be useful later, we recall that the first column Q_1 of matrix Q is the normalized eigenvector associated with the zero eigenvalue of the Laplacian matrix, hence $Q_1 = \bar{\mathbf{1}}/\sqrt{N}$.

Since we can also write

$$M = DD^\top = P[\ 0\ \Omega\ ][\ 0\ \Omega\ ]^\top P^\top = P\Omega^2 P^\top, \tag{9}$$

the eigenvalues of matrix M are all the nonzero eigenvalues of L (i.e., the diagonal entries of Ω^2).

With a few algebraic manipulations, the overall system can be written in matrix form as

$$\ddot{y} = -kLy - hL\dot{y} - r\dot{y} + r\bar{\mathbf{1}}v(t) + \Delta, \tag{10}$$

where $\Delta = \begin{bmatrix}\delta_1 \dots \delta_N\end{bmatrix}^\top$. To derive the dynamics of the average position a, let us pre-multiply Eq. (10) by $\bar{\mathbf{1}}^\top/N$:

$$\frac{1}{N}\bar{\mathbf{1}}^\top\ddot{y} = -\frac{k}{N}\bar{\mathbf{1}}^\top Ly - \frac{h}{N}\bar{\mathbf{1}}^\top Ly\ - \frac{r}{N}\bar{\mathbf{1}}^\top\ \dot{y} + \frac{r}{N}\bar{\mathbf{1}}^\top\bar{\mathbf{1}}v(t) + \frac{1}{N}\bar{\mathbf{1}}^\top\Delta \tag{11}$$

Then, in view of Eq. (6) and since $\frac{1}{N}\bar{\mathbf{1}}^\top y = a$ and $\bar{\mathbf{1}}^\top\bar{\mathbf{1}} = N$, we get

$$\ddot{a}(t) = -r\dot{a}(t) + rv(t) + \frac{1}{N}\bar{\mathbf{1}}^\top\Delta. \tag{12}$$

Hence, the dynamics of the average position does not depend on k and h, while it does depend on the reference speed v, on the design parameter r and on the average components of the disturbance:

$$\Delta_{av} \doteq \frac{1}{N}\bar{\mathbf{1}}^\top\Delta.$$

Note that the effect of the average disturbance Δ_{av} does not affect the inter-vehicle spacing, since it changes the average position, namely it moves all the vehicles of the same amount.

To derive the dynamics of the differences $z = Dy$, let us pre-multiply Eq. (10) by matrix D. Since $L = D^\top D$, we have

$$(D\ddot{y}) = -kDD^\top(Dy) - hDD^\top(D\dot{y}) - r(D\dot{y}) + rD\bar{\mathbf{1}}v(t) + D\Delta.$$

Then, in view of Eq. (5) and since $M = DD^\top$, we have

$$\ddot{z} = -kMz - hM\dot{z} - r\dot{z} + D\Delta. \tag{13}$$

Hence, the dynamics of the differences z does not depend on the reference speed $v(t)$, which can thus be changed as needed, without altering the dynamics of the system or hampering its safety. Also, it does not depend on the design parameter r and it only depends on the design parameters k and h, and on the component of the disturbance that is orthogonal to the average. As we will see later, the system in Eq. (13) is asymptotically stable; therefore, in the absence of disturbances, $z(t)$ converges to 0 as desired. In the presence of disturbances due to packet losses, instead, z can grow; however, it is fundamental to keep it bounded, since high values of the components of z (precisely, $z_i \leq -d$ for at least some i) mean that a collision has occurred.

The overall system can now be analyzed by separately studying the evolution of Eq. (12) and of Eq. (13). Interestingly, also the choice of the design parameters can be "decoupled", since r only affects the dynamics of the average a, while h and k only affect the dynamics of the differences z. In the following, Section 3.2 investigates the average properties of the platoon, while Section 3.3 explores the performance in terms of the differential dynamics between vehicles. We also briefly discuss the error dynamics in Section 3.4.

3.2 The average dynamics

Investigating the average platoon dynamics allows us to provide a criterion to select the design parameter r.

We consider a transient from zero speed to the desired speed $v(t)$, which can be studied by considering the system in Eq. (12) with initial conditions $a(0) = \dot{a}(0) = 0$. This means that the platoon is at rest in an initial position (assumed to be position 0). Its solution yields the average position

$$a(t) = vt - \frac{v}{r} + \frac{v}{r}e^{-rt},$$

with average speed

$$\dot{a}(t) = v - ve^{-rt}$$

and average acceleration

$$\ddot{a}(t) = rve^{-rt}.$$

At the beginning, the acceleration is maximal and equal to rv. The time constant

$$\tau_a = \frac{1}{r} \tag{14}$$

can be controlled by choosing r based on the trade-off between promptness and comfort.

3.3 The difference dynamics

A smooth average behavior of a platoon is important, but the dynamics of the differences z_i is fundamental for safety and group behavior: $z_i = d$ means that two vehicles are at the double of the desired distance d, while $z_i = -d$ means collision! The key design specification is therefore

$$|z_i| \leq \alpha d, \tag{15}$$

where $0 < \alpha < 1$ is a safety coefficient. As an example, if $d = 10\,\text{m}$, then $\alpha = 0.2$ (20%) implies that the true distance must be between 8 m and 12 m.

In particular, in the following we will be able to give bounds of the form $\|z| \leq \beta$, where $\|z\| = \sqrt{\sum_i z_i^2}$ is the Euclidean norm. This implies that the bound on all distances is $|z_i| \leq \beta$. Then, we must keep a safety distance $d > \beta c_s$, where $c_s \geq 1$ is a safety coefficient.

In wireless vehicular control, disturbances are essentially originated by packet loss. If a packet is not received by a vehicle, then there is a lack of information on the positions of the preceding and/or following vehicles. The typical (indeed probably the only reasonable one, given the small beaconing time) assumption in this case is that the vehicles are at the same distance with the same speed as the last transmitted information. The discrepancy between the actual relative position and speed and the estimated ones introduces a disturbance. Denoting by $\underline{y}_i$ the stale old information Eq. (2) yields

$$\begin{aligned} \ddot{y}_i = &-k(y_i - \underline{y}_{i+1} - d) - k(y_i - \underline{y}_{i-1} - d) \\ &- h(\dot{y}_i - \underline{\dot{y}}_{i+1}) - h(\dot{y}_i - \underline{\dot{y}}_{i-1}) - r(\dot{y}_i - \underline{v}). \end{aligned} \tag{16}$$

We can rewrite the dynamics as

$$\begin{aligned} \ddot{y}_i = &-k(y_i - y_{i+1} - d) - k(y_i - y_{i-1} - d) \\ &- h(\dot{y}_i - \dot{y}_{i+1}) - h(\dot{y}_i - \dot{y}_{i-1}) - r(\dot{y}_i - v) + \delta_i, \end{aligned} \tag{17}$$

where

$$\delta_i = h\frac{d}{dt}\delta y_{i+1} + h\frac{d}{dt}\delta y_{i-1} + k\delta y_{i+1} + k\delta y_{i-1} + r\delta v. \tag{18}$$

Equation (18) gives a clear criterion to co-design the parameters h and k and the communication system to keep the error within safe boundaries: Once a packet loss has occurred, we can investigate how the system recovers after the occurrence and how the system behaves if the packet losses occur repeatedly in a burst, leading to a potentially larger difference between the true information and the last received one.

Consider Eq. (13) and the perturbation term

$$D\Delta = \sqrt{2}\frac{D}{\sqrt{2}}\Delta.$$

It is not difficult to see that the entries of $D\Delta$ are the projections of Δ on the differences: for instance, $[1 \ -1 \ 0 \ 0 \ \dots]\Delta$ is the projection of Δ on the subspace $z_2 = y_1 - y_2$. Since $M = P\Omega^2 P^\top$ in view of Eq. (9), if we pre-multiply Eq. (13) by $P^\top$ and we denote $\hat{\delta} = P^\top D\Delta$, we get

$$P^\top \ddot{z} = -kP^\top P\Omega^2 P^\top z - hP^\top P\Omega^2 P^\top z - rP^\top \dot{z} + \hat{\delta},$$

hence

$$P^\top \ddot{z} = -k\Omega^2 P^\top z - h\Omega^2 P^\top z - rP^\top \dot{z} + \hat{\delta}.$$

Let us introduce the new variable

$$x = P^\top z,$$

to diagonalise the system, so that it is easier to study its stability. Recall that P is the orthonormal matrix such that $M = P\Omega^2 P^\top$ and the diagonal entries of $\Omega^2 = \mathrm{diag}\{\Omega_1^2, \dots, \Omega_{N-1}^2\}$ are the eigenvalues of M (i.e., the nonzero eigenvalues of L). It is important to stress that, since P is orthonormal, it does not change the Euclidean norm. Hence, $\|\hat{\delta}\| = \|P^\top D\Delta\| = \|D\delta\|$ and $\|x\| = \|P^\top z\| = \|z\|$.

Then, Eq. (13) can be rewritten as

$$\ddot{x} = -k\Omega^2 x - h\Omega^2 \dot{x} - r\dot{x} + \hat{\delta}. \tag{19}$$

If we apply the Laplace transform, with zero initial conditions, we have

$$X(s) = [s^2 I + (h\Omega^2 + rI)s + k\Omega^2]^{-1}\hat{\Delta}(s) = \Gamma(s)\hat{\Delta}(s),$$

where $\Gamma(s)$ is a diagonal matrix of transfer functions

$$\Gamma(s) = \text{diag}\left\{ \frac{1}{s^2 + (h\Omega_i^2 + r)s + k\Omega_i^2} \right\}.$$

The denominators of the transfer functions $\Gamma_i(s)$ are second order polynomials with positive coefficients, hence stability is ensured because their roots (the poles of the transfer functions) have a negative real part.

For simplicity, we assume the following.

Assumption 1 *The poles of the transfer functions $\Gamma_i(s)$ are real (and negative).*

With a suitable choice of the design parameters, we can make sure that the above assumption is always satisfied. In fact, we can prove the following result.

Proposition 1 *Assumption 1 is satisfied if*

$$h > \frac{k}{r}. \tag{20}$$

Proof. The discriminants of the second order polynomials at the denominator of $\Gamma_i(s)$ are $\Delta_{G_i} = (h\Omega_i^2 + r)^2 - 4k\Omega_i^2$. The roots of these polynomials are real provided that $\Delta_{G_i} > 0$. If $rh > k$, then

$$\begin{aligned} \Delta_{G_i} &= h^2\Omega_i^4 + r^2 + 2rh\Omega_i^2 - 4k\Omega_i^2 \\ &> h^2\Omega_i^4 + r^2 + 2rh\Omega_i^2 - 4rh\Omega_i^2 \\ &= (h\Omega_i^2 - r)^2 \\ &> 0. \end{aligned} \tag{21}$$

■

Hence, to guarantee that the poles of the transfer functions $\Gamma_i(s)$ are real and negative, it is enough to assume that Eq. (20) holds.

Under this assumption, we now consider two problems:

1. the reaction of the platoon to an erroneous position of one of more vehicles (with no disturbances);

2. the reaction of the platoon to disturbances that are bounded in norm as $\|\hat{\delta}\| \leq \rho$.

For the first problem, we assume that $D\Delta = 0$ and that at some time ($t = 0$ without loss of generality) there is a mismatch in the position: $z(0) = z_0$, with zero speed. Then, we consider the Laplace transform: since $\mathcal{L}[z(t)] = Z(s)$, $\mathcal{L}[\dot{z}(t)] = sZ(s) - z_0$ and $\mathcal{L}[\ddot{z}(t)] = s^2Z(s) - sz_0$, from Eq. (13) we get

$$[s^2I + (hM + rI)s + kM]Z(s) = [sI + (hM + rI)]z_0, \tag{22}$$

where for simplicity we drop the subscript in the $(N-1) \times (N-1)$ identity matrix $I = I_{N-1}$. By exploiting the equalities $I = PP^\top$ and $M = P\Omega^2P^\top$, we get

$$P[s^2I + (h\Omega^2 + rI)s + k\Omega^2]P^\top Z(s) = P[sI + (h\Omega^2 + rI)]P^\top z_0.$$

Since $X(s) = P^\top Z(s)$ and $x_0 = P^\top z_0$,

$$\begin{aligned} X(s) &= [s^2I + (h\Omega^2 + rI)s + k\Omega^2]^{-1}[sI + (h\Omega^2 + rI)]x_0 \\ &\doteq \Phi(s)x_0 = \mathrm{diag}\left\{\frac{s + (h\Omega_i^2 + r)}{s^2 + (h\Omega_i^2 + r)s + k\Omega_i^2}\right\}x_0. \end{aligned}$$

Then, the components of x evolve independently. Let us consider the inverse transform $\phi(t) = \mathrm{diag}\{\phi_i(t)\} = \mathcal{L}^{-1}[\Phi(s)]$. We have that $\phi_i(0) = 1$, from the initial value theorem ($\lim_{t\to 0}\phi_i(t) = \lim_{s\to\infty} s\Phi_i(s)$). Hence $\phi(0) = I$. Moreover, all $\phi_i(t)$ are strictly decreasing, as can be shown by considering their derivative:

$$\begin{aligned} \mathcal{L}[\dot{\phi}_i(t)] &= s\Phi_i(s) - \phi_i(0) \\ &= s\frac{s + (h\Omega_i^2 + r)}{s^2 + (h\Omega_i^2 + r)s + k\Omega_i^2} - 1 \\ &= \frac{-k\Omega_i^2}{s^2 + (h\Omega_i^2 + r)s + k\Omega_i^2}. \end{aligned}$$

This transfer function has real poles only, no zeros, and a negative coefficient at the numerator, hence its inverse Laplace transform $\dot{\phi}_i(t)$ is negative [28,29]. Hence, all $\phi_i(t)$'s are equal to 1 at $t = 0$ and converge to 0 for $t \to \infty$ (because the poles of the transfer function are real and negative). Therefore, they must be always positive and bounded as $\|\phi(t)\| \leq 1$ for all t. Hence, $|x_i(t)| < |x_{0,i}|$ for $t > 0$. Coming back to z, the inverse transform of $Z(s)$ is $z(t) = P\phi(t)P^\top z_0$. Hence, for a perturbation of size $\|z_0\|$,

$$\|z(t)\| = \|P\phi(t)P^\top z_0\| = \|\phi(t)\|\|z_0\| < \|z_0\|, \quad \text{for} \quad t > 0. \tag{23}$$

The previous inequality ensures string stability. Assume there is a misplacement (error) measured by $|z_i(0)|= \zeta$, then $\|z_0\|= \zeta$, this implies that $\|z(t)\|< \zeta$. Since the norm is greater or equal than the magnitude of any component, then $|z_j(t)|\leq \zeta$: no component will exceed the initial size ζ. More formally:

Proposition 2 *If $z_i(0) = \zeta \neq 0$ and $z_j(0) = 0$ for $j \neq i$, then $|z_j(t)|\leq \zeta$ for $t > 0$.*

To determine the effect of a nonzero disturbance Δ, we can consider Eqs. (13) and (19) indifferently, since the transformation $P^\top$ is norm-preserving. Consider Eq. (19), namely

$$\ddot{x} = -k\Omega^2 x - h\Omega^2 \dot{x} - r\dot{x} + \hat{\delta},$$

and assume that $\hat{\delta}(t)$ is bounded in norm as $\|\hat{\delta}(t)\|\leq \rho$. The transfer function for this system is $\Gamma(s)$, hence

$$X(s) = \Gamma(s)\hat{\Delta}(s).$$

If we assume zero initial conditions and consider the inverse Laplace transform $\gamma(t) = \mathcal{L}^{-1}[\Gamma(s)]$, the solution is given by the convolution

$$x(t) = \int_0^t \gamma(\sigma)\ \hat{\delta}(t-\sigma)d\sigma.$$

Then

$$\begin{aligned}
\|x(t)\| &= \left\| \int_0^t \gamma(\sigma)\ \ \hat{\delta}(t-\sigma)d\sigma \right\| \\
&\leq \int_0^t \|\gamma(\sigma)\|\|\hat{\delta}(t-\sigma)\|d\sigma \leq \rho \int_0^t \|\gamma(\sigma)\|d\sigma \\
&\leq \rho \int_0^\infty \|\gamma(\sigma)\|d\sigma = \rho \max_k \int_0^\infty |\gamma_k(\sigma)|d\sigma = \rho \max_k \int_0^\infty \gamma_k(\sigma)d\sigma.
\end{aligned}$$

We removed the absolute value because $\gamma_k(\sigma)$ is a positive function. In fact, it has real poles only, no zeros and a positive coefficient at the numerator [28,29]. The value of the integral can be computed by means of the final value theorem:

$$\int_0^\infty \gamma_k(\sigma)d\sigma = \left. \frac{1}{s^2 + (h\Omega_i^2 + rI)s + k\Omega_i^2} \right|_{s=0} = \frac{1}{k\Omega_i^2}.$$

This results in the bound

$$\|x(t)\| \leq \rho \frac{1}{k\Omega_1^2},$$

where Ω_1^2 is the smallest eigenvalue of M (i.e., the smallest nonzero eigenvalue of L). Recall that $\|x(t)\| = \|z(t)\|$.

As a final consideration, the error given by Eq. (18) scales with k, h and r, if we assume that v is fixed and exactly known. On the other hand, Eq. (20) is assumed to hold, hence $hr > k$. If we take $h/k = (1+\epsilon)/r$, with $\epsilon > 0$, the overall error scales linearly with k, because we can write

$$\begin{aligned}
\|\delta_i\| &= k \left\| \frac{h}{k}\frac{d}{dt}\delta y_{i+1} + \frac{h}{k}\frac{d}{dt}\delta y_{i-1} + \delta y_{i+1} + \delta y_{i-1} \right\| \\
&= k \left\| \frac{1+\epsilon}{r}\frac{d}{dt}\delta y_{i+1} + \frac{1+\epsilon}{r}\frac{d}{dt}\delta y_{i-1} + \delta y_{i+1} + \delta y_{i-1} \right\| \\
&\leq k\delta_{M_i},
\end{aligned}$$

hence, since $\|\hat{\delta}\| = \|P^\top D\Delta\|$ and $\|D\| \leq 2$,

$$\|\hat{\delta}(t)\| \leq 2k\delta_M \doteq \rho, \tag{24}$$

where δ_M is a bound for the cumulative error of position and speed (according to some norm). Then, we get the bound

$$\|x(t)\| \leq \frac{2\delta_M}{\Omega_1^2}, \tag{25}$$

which depends uniquely on the eigenvalue Ω_1^2.

3.4 The error dynamics

We briefly discuss here the dynamics of the error variable e, defined as

$$e = y - \bar{\mathbf{1}}\frac{\bar{\mathbf{1}}^\top y}{N} = [I - \frac{\bar{\mathbf{1}}\bar{\mathbf{1}}^\top}{N}]y.$$

The ith component of vector e is the difference between y_i and the average $a = \frac{\bar{\mathbf{1}}^\top y}{N}$:

$$e_i = y_i - \frac{\bar{\mathbf{1}}^\top y}{N} = y_i - \frac{1}{N}\sum_{j=1}^{N} y_j.$$

Consider Eq. (10) and pre-multiply it by $[I-\frac{\bar{\mathbf{1}}\bar{\mathbf{1}}^\top}{N}]$. Since $[I-\frac{\bar{\mathbf{1}}\bar{\mathbf{1}}^\top}{N}]L = L[I-\frac{\bar{\mathbf{1}}\bar{\mathbf{1}}^\top}{N}]$ and $[I-\frac{\bar{\mathbf{1}}\bar{\mathbf{1}}^\top}{N}]\bar{\mathbf{1}} = 0$, we get

$$\begin{aligned}
\ddot{e} &= [I-\frac{\bar{\mathbf{1}}\bar{\mathbf{1}}^\top}{N}]\ddot{y} \\
&= -k[I-\frac{\bar{\mathbf{1}}\bar{\mathbf{1}}^\top}{N}]Ly - h[I-\frac{\bar{\mathbf{1}}\bar{\mathbf{1}}^\top}{N}]L\dot{y} - r[I-\frac{\bar{\mathbf{1}}\bar{\mathbf{1}}^\top}{N}]\dot{y} \\
&\quad +[I-\frac{\bar{\mathbf{1}}\bar{\mathbf{1}}^\top}{N}]r\bar{\mathbf{1}}v(t) + [I-\frac{\bar{\mathbf{1}}\bar{\mathbf{1}}^\top}{N}]\Delta \\
&= -kLe - (hL+rI)\dot{e} + \Delta_{err}
\end{aligned}$$

where $\Delta_{err} \doteq [I-\frac{\bar{\mathbf{1}}\bar{\mathbf{1}}^\top}{N}]\Delta$. Note that the evolution of the error variable does not depend on v.

We now show that the variance $\|e\|/\sqrt{N}$ is decreasing. Let e_0 be a nonzero initial condition and $\Delta_{err} = 0$. Then, in the Laplace transform domain,

$$[s^2I + (hL+rI)s + kL]E(s) = [sI + (hL+rI)]e_0. \tag{26}$$

Adopting the decomposition Eq. (8) and repeating the same procedure as in the previous sections,

$$E(s) = Q[s^2I + (h\Lambda^2+rI)s + k\Lambda^2]^{-1}[sI + (h\Lambda^2+rI)]Q^\top e_0,$$

where $\Lambda^2 = \mathrm{diag}\{0, \Omega^2\}$. Define the diagonal transfer function matrix

$$\Psi(s) = \mathrm{diag}\left\{\frac{s+(h\Lambda_i^2+r)}{s^2+(h\Lambda_i^2+r)s+k\Lambda_i^2}\right\},$$

whose first diagonal term is equal to $1/s$, because the first eigenvalue of the Laplacian L is $\Lambda_1 = 0$, while the other diagonal terms are the same as those in $\Phi(s)$:

$$\Psi(s) = \mathrm{diag}\left\{\frac{1}{s}, \Phi(s)\right\}.$$

Hence, along the same lines as in the derivation for z, denoting by $\psi(t)$ the inverse Laplace transform of $\Psi(s)$, we get

$$e(t) = Q\psi(t)Q^\top e_0. \tag{27}$$

Note that $\psi(t)$ has the same diagonal entries as $\phi(t)$ and an extra diagonal entry (the first) that is equal to 1: $\psi_{11}(t) = 1$. Therefore, we can conclude

that $\|e(t)\|$ is non-increasing. Now, we observe that an initial condition e_0 is meaningful if it has 0 mean. The first row of $Q^\top$ is equal to $\bar{\mathbf{1}}^\top/\sqrt{N}$, the eigenvector associated with the 0 eigenvalue of L, hence the constant term associated with the mode $\psi_{11}(t) = 1$ disappears in Eq. (27). This proves that the variance $\|e(t)\|/\sqrt{N}$ is indeed decreasing and converges to 0 as t grows large.

4 Mapping Packet Losses to Error Bounds

In cooperative driving the loss of packets is by far the major source of disturbance: delays are negligible with direct communications, and sensor errors are limited; the loss of consecutive packet instead means that the controller is "blinded" for hundreds of milliseconds. Let N_L be the maximum number of consecutive losses (burst) than can occur in the channel with a certain probability bound. Above this value the network is faulty, and the system should enter a disaster recovery phase, which is out of the scope of this paper.

For the worst-case analysis we want to compute the bound imposed by the loss of N_L consecutive packets on the disturbance term δ_i; we consider the error in Eq. (18). The error is expressed as the sum of the position, speed, and reference speed errors multiplied by their coefficients. With respect to the position and the speed error, the upper bound can be computed by considering the maximum jerk $\bar{j}$ (the derivative of acceleration) a vehicle can implement. We compute the bounds on position and speed error as

$$\bar{\delta}^{\dot{y}} = \int_0^{(N_L+1)T} \int_0^t \bar{j} dt\, dt = \frac{\bar{j}}{2} \left((N_L+1)T\right)^2 \tag{28}$$

$$\bar{\delta}^{y} = \int_0^{(N_L+1)T} \int_0^t \int_0^t \bar{j} dt\, dt\, dt = \frac{\bar{j}}{6} \left((N_L+1)T\right)^3, \tag{29}$$

where T is the packet transmission interval. With respect to the reference speed error, the bound depends on how much the reference can change. In cruising conditions sharp changes of reference are not needed and we set a maximum allowed change in reference speed named $\bar{v}$ between consecutive packets. By combining Eqs. (18), (28) and (29) we obtain the error bound

$$\delta_M = 2\left(h\frac{\bar{j}}{2}\left((N_L+1)T\right)^2 + k\frac{\bar{j}}{6}\left((N_L+1)T\right)^3\right) + r\bar{v}\cdot(N_L+1). \tag{30}$$

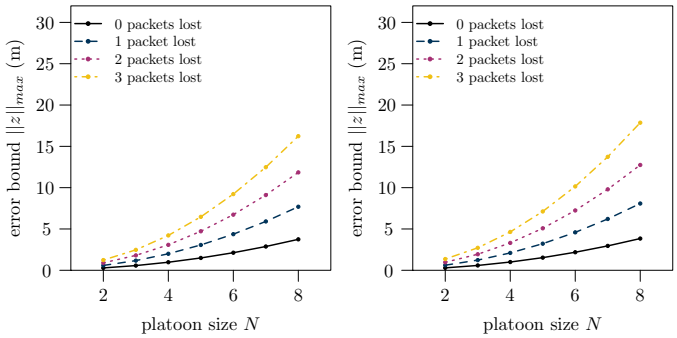

(a) $\bar{j} = 1\,\mathrm{m/s^3}$ (b) $\bar{j} = 2\,\mathrm{m/s^3}$

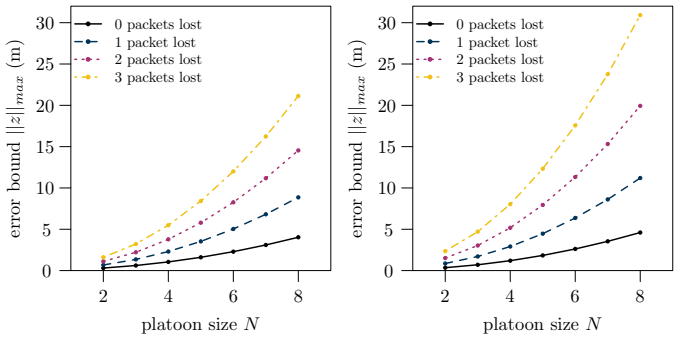

(c) $\bar{j} = 4\,\mathrm{m/s^3}$ (d) $\bar{j} = 10\,\mathrm{m/s^3}$

Figure 1: Error bound $\|z\|_{max}$ as function of the platoon size N, for different maximum jerks $\bar{j}$ and burst size N_L.

It is necessary to double the position and speed error bounds to consider both preceding and following vehicles. Finally, to compute the maximum possible error we consider the smallest non-zero eigenvalue Ω_1^2 of $L = D^\top D$, computed using the singular value decomposition of matrix D, and we exploit the fact that $\|z\| \leq \frac{2\delta_M}{\Omega_1^2}$, in view of Eq. (25) and of the fact that $\|x\| = \|z\|$. Note that the value Ω_1^2 depends on the number of vehicles: the larger the number of vehicles, the smaller Ω_1^2. Finally, we set the inter-vehicle distance to

$$d > \frac{2\delta_M}{\Omega_1^2} c_s, \tag{31}$$

where $c_s \geq 1$ is a safety coefficient.

Figure 1 plots the bound $\|z\|_{max} = \frac{2\delta_M}{\Omega_1^2}$ and, thus, the minimum safety

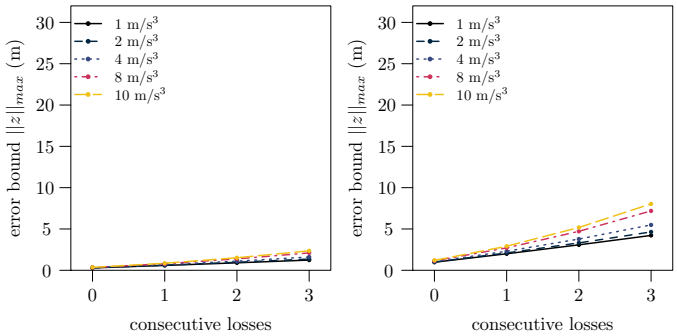

(a) 2 vehicles (b) 4 vehicles

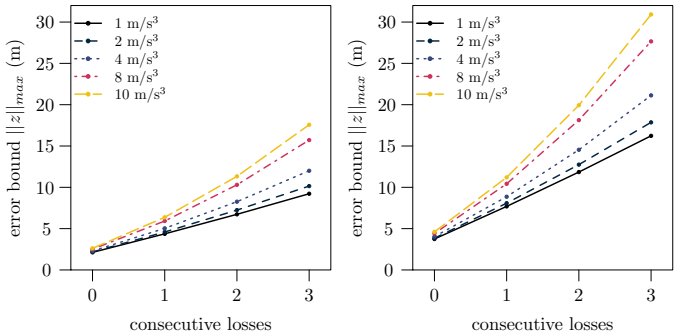

(c) 6 vehicles (d) 8 vehicles

Figure 2: Error bound $\|z\|_{max}$ as function of the number of consecutive packet losses N_L, for different platoon sizes N and maximum jerks $\bar{j}$.

distance d as a function of the platoon size N, for different maximum jerks $\bar{j}$ and number of consecutive losses N_L. The remaining parameters are fixed: $T = 100\,\text{ms}$, $\bar{v} = 1\,\text{km/h}$ per packet[1], $k = 0.5$, $h = 0.71$, $r = 1$. The platoon size N has the largest impact, as the bound grows more than linearly with N. The parameters N_L and $\bar{j}$ also play a significant role, but the impact is not as large. In good network conditions the control system is definitely performing well, as the worst-case upper bound is below 3 m even with 8 vehicles. In non-ideal network conditions, instead, there is an important trade-off in the choice of the parameters. To have small inter-vehicle distances, we either need to ensure a high network reliability (thus, a low N_L) or limit the size

[1] This corresponds to 10 km/h per second with the given T, which is much more than the normal speed change we expect while cruising.

of the platoon. Indeed, this allows us to easily regulate d and dynamically adapt it to the network condition. Otherwise, the performance of the vehicle can also be considered and, if needed, altered for system tuning. For example, by limiting the maximum jerk to $4\,\mathrm{m/s^3}$ the system can maintain a relatively small distance while being robust to heavy packet losses. This is also shown in Fig. 2, where we plot the bound $\|z\|_{max}$ as function of the number of consecutive losses N_L. It is important to remember that the bound $\|z\|_{max}$ is computed as a worst-case which, in reality, might never occur. In the next section we show that the norm of the distance errors in realistic conditions is much smaller than the bound $\|z\|_{max}$.

5 Performance Evaluation

We implement the proposed control system in the platooning simulator PLEXE [30], which allows us to test the performance of platooning control algorithms under realistic vehicle dynamics and communication models. It is especially valuable for assessing implementation-related issues as, e.g., the effect of asynchronous control data. As the data exchange rate (10 Hz) between vehicles is slower than the actuation control loop (100 Hz [4]) and vehicles might not be synchronized, the data provided to the algorithm might be incoherent from a time perspective. As an example, the own GPS position might be up to date, while the position of the front and back vehicles is "frozen" to the value included within the last received beacon.

To cope with this issue the control system includes a predictor, which computes missing values by interpolation. More formally, assume that $\ddot{y}_{t_0}$, $\dot{y}_{t_0}$, and y_{t_0} are the acceleration, speed, and position of a vehicle at time t_0. To estimate speed and position of such vehicle at the current time t, the control system computes

$$\dot{y}_t = \dot{y}_{t_0} + \ddot{y}_{t_0}\,(t - t_0)\,, \quad y_t = y_{t_0} + \frac{t - t_0}{2}\,(\dot{y}_t + \dot{y}_{t_0})\,. \tag{32}$$

The use of Eq. (32) makes PLEXE simulation extremely realistic as this is what on-board controllers are expected to do.

5.1 Error Dynamics Comparison

We first show the dynamics of the vehicles without network impairments. The goal is to understand the behavior of the controller, which is qualitatively

different from the solutions proposed in the literature. We compare our algorithm with the controller designed in [4], which is a well-known CACC using a time headway spacing policy.

Figure 3 shows the distance error dynamics between vehicles V_i and V_{i-1} for a platoon of 8 cars under a sinusoidal disturbance. For the CACC designed by Ploeg et. al., the leader changes its speed following the sinusoidal pattern, while for our controller we change the reference speed v. Figure 3a shows the classical attenuation of the error dynamics towards the tail of the platoon, thanks to the string-stability property. Our approach (Fig. 3b) is string stable as well, but the maximum attenuation occurs at the middle of the platoon and the dynamics are symmetric with respect to the center.

We can make an analogy between our algorithm and a spring-damper system (Fig. 5). We can imagine that consecutive vehicles are connected through a spring, and an additional spring which represents the reference speed v. When changing the reference speed the vehicles are pushed back/pulled forward all at the same time, and the "inner" springs take care of attenuating the internal errors. A non trivial consequence of this controller structure is that position errors are compensated balancing the control effort between the front and rear vehicle, while in most other controllers the effort is all on the rear vehicle. This is in line with the "philosophy" of an autonomous driving platoon and not of a human-driven vehicle followed by partially automated vehicles. Further discussion on this topic is beyond the scope of this paper.

5.2 Error Bound Analysis.

As a second analysis we perform a set of simulations to empirically show that the error bound computed in Section 3.3 is always respected. To this aim, we implement a scenario where the leader vehicle continuously changes the reference speed v by an amount $\bar{v}$ for each packet (i.e., every T seconds). In addition, we consider a channel causing burst losses at the receivers. In particular, each received packet has a certain probability of triggering a burst of losses. If a burst is triggered, the vehicle discards all the incoming packets received until the time $n_L T$ has elapsed, loosing n_L consecutive packets for each vehicle. n_L is drawn from a discrete uniform distribution $\mathcal{U}(1, N_L)$. After the end of a burst, each receiver waits a minimum amount of time before starting the next one. The analysis on the bound is indeed valid when considering the system at steady state. After a burst of losses, the system needs a certain amount of time to converge (cf. Eq. (14)) to eliminate the

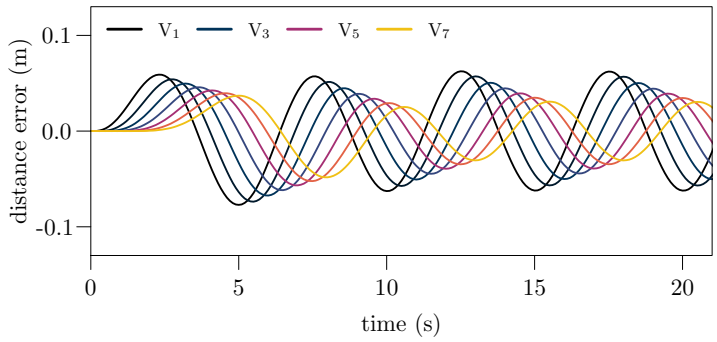

(a) CACC in [4]

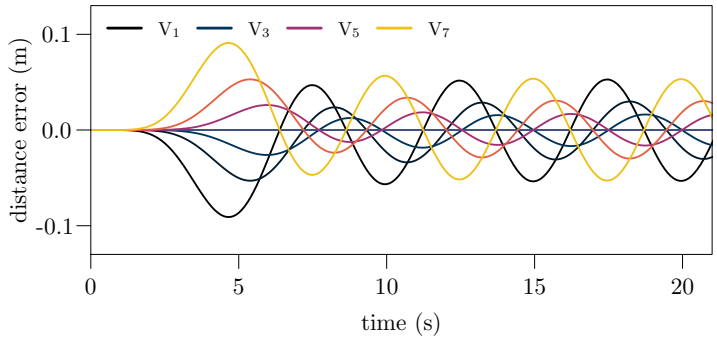

(b) Our proposal ($N = 8$)

Figure 3: Qualitative comparison between a classic algorithm and the proposed solution (distance errors under a sinusoidal disturbance).

accumulated error. However, we also consider very small network up-times (as small as 100 ms) to show the robustness of our approach. Finally, we consider first order actuation lag with a time constant $\tau = 0.5\,\mathrm{s}$, i.e., the response of the engine and the braking system to actuation commands $\ddot{y}$ is modeled by the following transfer function $\ddot{y}_{\mathrm{real}} = \dfrac{1}{\tau s + 1}\ddot{y}$, which is a common and verified assumption [4, 6–8]. Table 2 summarizes simulation parameters.

For each simulation s, we compute the norm of the error vector as

$$\|z_s\| = \max_k \sqrt{\sum_{i=1}^{N} (d_{k,i} - d)^2}, \tag{33}$$

where $d_{k,i}$ is the distance between vehicles V_i and V_{i-1} at simulation step k

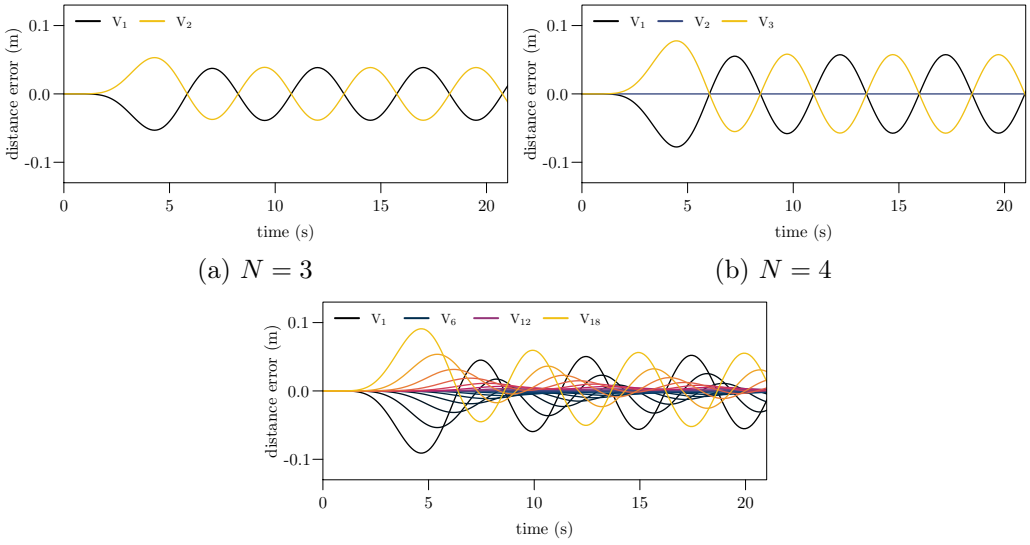

(a) $N = 3$ (b) $N = 4$

(c) $N = 19$

Figure 4: Distance errors dynamics for the proposed approach under a sinusoidal disturbance for different number of vehicles.

and d is the target distance. We then verify that $\|z_s\| \leq \|z\|_{max}$ for all the simulations, where $\|z\|_{max}$ is the theoretic bound for the norm, computed upon the parameters chosen for that particular simulation.

In the computation of the theoretic bound, however, the maximum jerk $\bar{j}$ is not clearly defined. In the real world it can either be a physical limit of the engine or the braking system, or a design parameter. In the simulations there is no such limit. For this reason, we post-analyze the maximum jerks obtained in the simulations. Figure 6 shows an histogram of the maximum jerk value of each simulation. Small maximum jerks ($1.5\,\mathrm{m/s^3}$ to $3.5\,\mathrm{m/s^3}$) occur when packet loss events are unlikely and for small values of the r parameter. Recall that r balances the trade-off between settling time and driving comfort, so a higher value is more likely to cause large acceleration changes. Medium jerk values ($5.5\,\mathrm{m/s^3}$ to $8\,\mathrm{m/s^3}$) are caused by a large value of the r parameter ($r = 4$), or a small r value combined with moderate packet losses. Finally, heavy losses cause large maximum jerk values, as the system obtains control data after long periods of silence, requiring strong actions to compensate the error. To compute the theoretic error bounds we use the minimum of the values shown in Fig. 6, i.e., $1.5\,\mathrm{m/s^3}$.

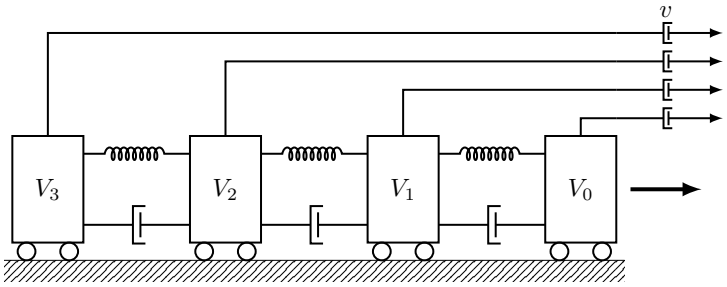

Figure 5: Spring-damper representation of the proposed control system.

Table 2: Simulation parameters.

Parameter	Value
k, h, T, τ	0.5, 0.71, 100 ms, 0.5 s
r	$\sqrt{0.5}$, 1, 4
n_L	1, $\sim\mathcal{U}(1,3)$, $\sim\mathcal{U}(1,5)$
Start burst probability	1 %, 5 %, 10 %, 20 %, 30 %, 40 %, and 50 %
Minimum no-burst time	0.1 s, 0.3 s, 0.5 s, 1 s, and 3 s
$\bar{v}$	1 km/h per packet
Repetitions	10

Figure 7 plots the simulation and theoretic bounds for different combinations of the r and N_L parameters. Simulation bounds are marked with points, while theoretic bounds are marked with crosses. The graph clearly shows that the theoretic bounds are respected. The margin between simulation and theory is large and this is due to two facts.

First, the bound $\|z\|_{max}$ is computed on the worst case: a change in the reference speed, a burst loss of N_L packets, and a change in the dynamics with the maximum jerk should occur at the same time. This is very unlikely even in a synthetic scenario like the one we consider, especially because the jerk is a consequence of the control action computed by the algorithm.

Second, the predictor implemented within the control system counteracts the effects of packet losses, estimating the position and the speed of other vehicles during network down time. The effectiveness of the predictor is evident, as the impact of the burst length is smaller compared to the impact of r.

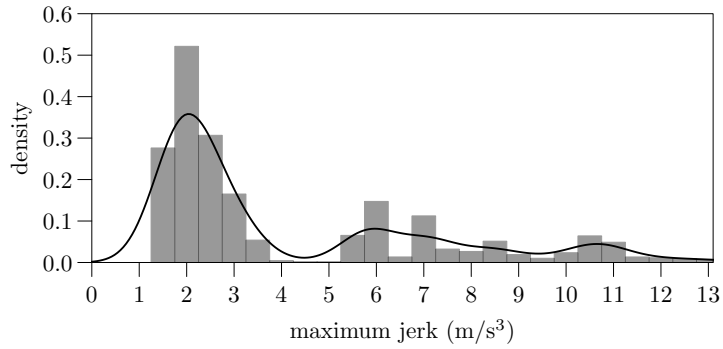

Figure 6: Distribution of maximum jerks measured over all simulation runs.

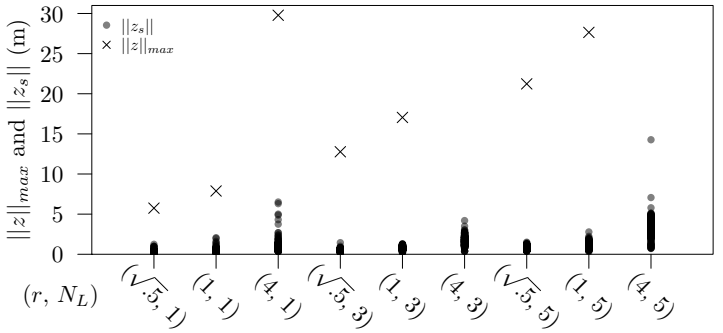

Figure 7: Plot of the simulation ($\|z_s\|$) and the theoretic ($\|z\|_{max}$) bounds, for different combinations of the r and N_L parameters. The $\|z\|_{max}$ values for $(r, N_L) = (1, 3)$ and $(4, 5)$ are out of scale and are not shown for the sake of clarity.

5.3 Emergency Braking

We tested the performance of the control system with respect to cruising, which is the main purpose of a platooning control algorithm. A platoon, however, is also required to react to emergencies and external inputs. One example is an emergency braking maneuver [31].

With "emergency braking" we refer here to the action of coming to a complete stop with a strong deceleration. For strong we mean a deceleration value which can be perceived as uncomfortable by a passenger, i.e., a value larger than $4\,\mathrm{m/s^2}$ [32]. Differently from conventional CACC systems, where the leader is controlled by an independent law, our design controls leader's behavior as well. Setting the reference speed $v = 0$ is not enough, as the algorithm smoothly converges to the desired speed with a comfortable

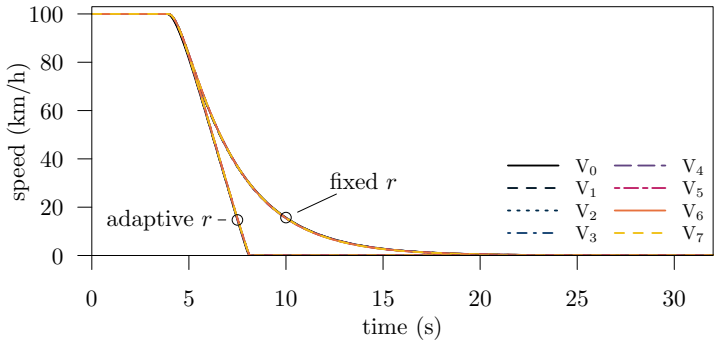

Figure 8: Comparison of the speed dynamics when setting the reference speed $v = 0\,\text{km/h}$ from $v = 100\,\text{km/h}$ with and w/o adaptive r.

deceleration and not in "emergency mode". To realize an emergency braking maneuver we thus need to modify controller parameters "on the fly", in particular by acting on the desired speed v and the vehicle-reference friction coefficient r. Let us assume that the leader is traveling at speed v_0. To implement the maneuver, we set $v = 0$ and $r = \frac{d_{\text{dec}}}{v_0}$, where d_{dec} is the desired deceleration. This causes the leader to start braking with a deceleration d_{dec} and progressively reduce the deceleration as its speed approaches 0. Figure 8 shows the comparison between the two approaches when choosing a strong desired deceleration of $8\,\text{m/s}^2$. When the leader sets the reference speed $v = 0$ ($5\,\text{s}$ simulation time), but does not adapt r the platoon takes $15\,\text{s}$ to come down to a complete stop, while when r is adapted to the situation of a sudden unforeseen stop the platoon comes to a complete stop in $3\,\text{s}$ to $4\,\text{s}$. The average behavior is always smooth and depends only hon how r is changed.

Figure 9 shows the differential dynamics of the maneuver in terms of relative vehicles distance in the same conditions of Fig. 8 in four different conditions: Without adapting r (Fig. 9a); without adapting r when the fourth vehicle V_3 initiates the maneuver (Fig. 9b); adapting r (Fig. 9c); and adapting r when the fourth vehicle V_3 initiates the maneuver (Fig. 9d). As expected, changing dynamically r allows a faster deceleration, but ends in larger deviation from d in inter-vehicles distance, that remain in any case in the order of tens of cm. Interestingly, if the stop is declared by a vehicle in the middle of the platoon, a feature this controller enables, distance errors are smaller. After the platoon comes to a complete stop, the vehicles keep moving very slowly to bring the inter-vehicle distance exactly to d, but these are movements of centimeters and vehicles can be conveniently stopped at

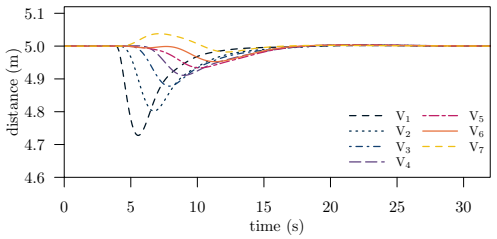

(a) No r adaptation, V_0 declares the stop

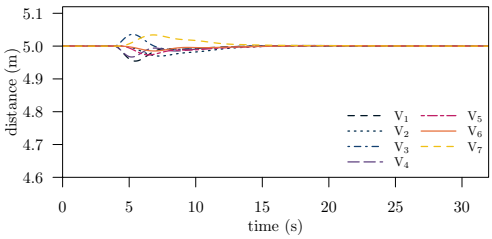

(b) No r adaptation, V_3 declares the stop

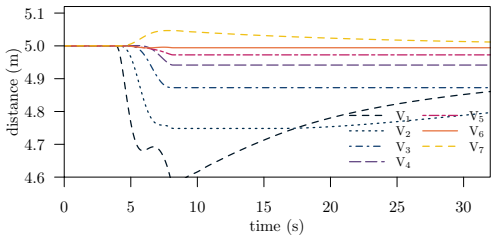

(c) Adapting r, V_0 declares the stop

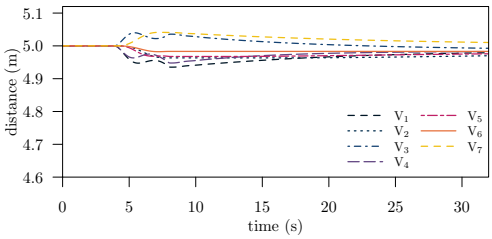

(d) Adapting r, V_3 declares the stop

Figure 9: Comparison of the relative vehicles' position when setting the reference speed $v = 0\,\text{km/h}$ from $v = 100\,\text{km/h}$ without adapting r when V_0 (a) and V_3 declare the stop, adapting r when V_0 (c) and V_3 (d) declare the stop.

any distance if desired.

An additional perspective on the dynamics of the manuever is given in Figs. 10 and 11. The figures show the desired acceleration and the real acceleration (post actuation) of the vehicles during the maneuver. It is clear that simply setting the reference speed $v = 0$ and r to obtain the desired deceleration value without adapting r simply generates a single "peak of deceleration", which smoothly converges to 0 following the speed profile. Conversely, the adaption of r maintains the deceleration roughly constant, correctly realizing the emergency maneuver.

One observation to make in this scenario is that the theoretic bound $\|z\|_{max}$ is not valid during the emergency maneuvers, as the parameters of the controller change and the scenario is no more a standard cruise, but an emergency stop. The platoon, however, remains very stable and distances, as shown by results, remain well within safety, and indeed within the "cruising bound", even if it is not theoretically valid.

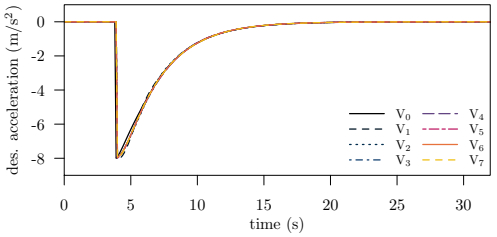

(a) No r adaptation, V_0 declares the stop

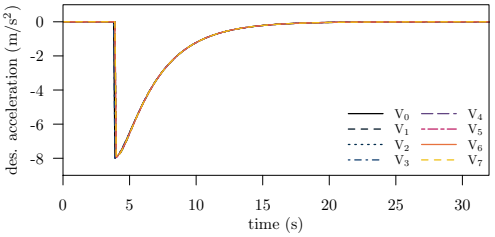

(b) No r adaptation, V_3 declares the stop

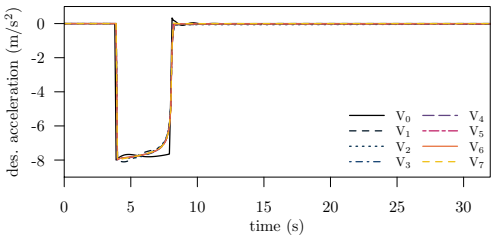

(c) Adapting r, V_0 declares the stop

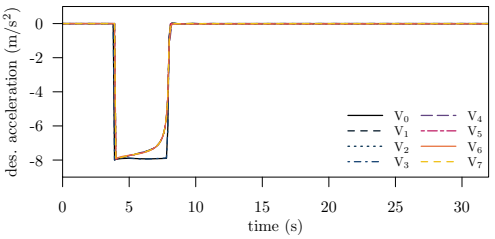

(d) Adapting r, V_3 declares the stop

Figure 10: Comparison of the control input (desired acceleration) profiles when setting the reference speed $v = 0\,\text{km/h}$ from $v = 100\,\text{km/h}$ without adapting r when V_0 (a) and V_3 declare the stop, adapting r when V_0 (c) and V_3 (d) declare the stop.

6 Concluding Discussion and Future Work

In this work we designed a cooperative automatic driving algorithm from a joint network and control perspective. We derived safety upper bounds on the inter-vehicle distance depending on vehicle dynamics and packet losses caused by network impairments, showing by means of simulations that such bounds are never violated. On the contrary, the bounds are respected with a large margin due to the robustness of the algorithm to packet losses. Hence, our future work aims at reducing the theoretic error bound by considering the effect of a predictor or, alternatively, at designing an adaptive message dissemination algorithm that reduces the broadcast rate depending on the need. The latter objective would permit to minimize network utilization while still guaranteeing the safety and the robustness to the system. To the best of our knowledge, this would be a significant achievement.

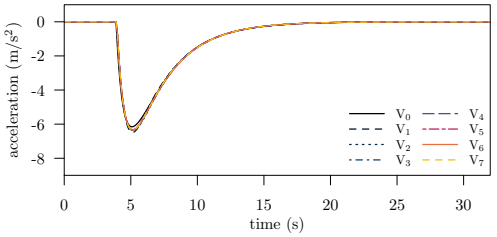

(a) No r adaptation, V_0 declares the stop

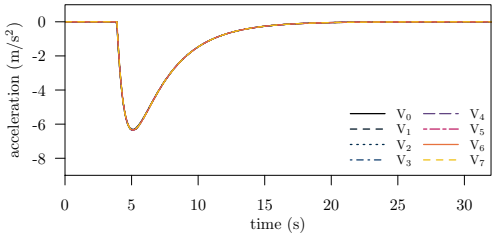

(b) No r adaptation, V_3 declares the stop

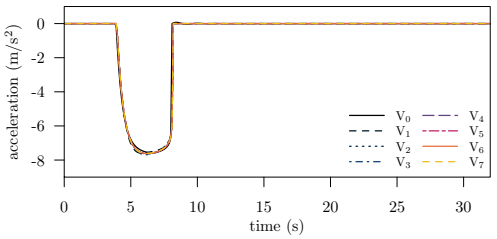

(c) Adapting r, V_0 declares the stop

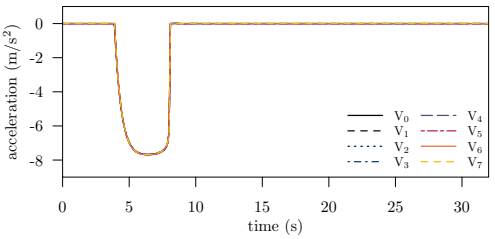

(d) Adapting r, V_3 declares the stop

Figure 11: Comparison of the acceleration profiles when setting the reference speed $v = 0\,\mathrm{km/h}$ from $v = 100\,\mathrm{km/h}$ without adapting r when V_0 (a) and V_3 declare the stop, adapting r when V_0 (c) and V_3 (d) declare the stop.

References

[1] B. van Arem, C. van Driel, and R. Visser, "The Impact of Cooperative Adaptive Cruise Control on Traffic-Flow Characteristics," *IEEE Transactions on Intelligent Transportation Systems*, vol. 7, no. 4, pp. 429–436, Dec. 2006.

[2] P. S. Jootel, "SAfe Road TRains for the Environment," SARTRE Project, Final Project Report, Oct. 2012.

[3] S. Singh, "Critical reasons for crashes investigated in the National Motor Vehicle Crash Causation Survey," National Center for Statistics and Analysis (NHTSA), Technical report DOT HS 812 115, Feb. 2015.

[4] J. Ploeg, B. Scheepers, E. van Nunen, N. van de Wouw, and H. Nijmeijer, "Design and Experimental Evaluation of Cooperative Adaptive Cruise Control," in *IEEE International Conference on Intelligent Transportation Systems (ITSC 2011)*. Washington, DC: IEEE, Oct. 2011, pp. 260–265.

[5] R. Kianfar, P. Falcone, and J. Fredriksson, "A Receding Horizon Approach to String Stable Cooperative Adaptive Cruise Control," in *14th International IEEE Conference on Intelligent Transportation Systems (ITSC 2011)*. Washington, DC: IEEE, Oct. 2011, pp. 734–739.

[6] V. Milanés, S. E. Shladover, J. Spring, C. Nowakowski, H. Kawazoe, and M. Nakamura, "Cooperative Adaptive Cruise Control in Real Traffic Situations," *IEEE Transactions on Intelligent Transportation Systems*, vol. 15, no. 1, pp. 296–305, Feb. 2014.

[7] R. Rajamani, *Vehicle Dynamics and Control*, 2nd ed. Springer, 2012.

[8] A. Ali, G. Garcia, and P. Martinet, "The Flatbed Platoon Towing Model for Safe and Dense Platooning on Highways," *Intelligent Transportation Systems Magazine, IEEE*, vol. 7, no. 1, pp. 58–68, Jan. 2015.

[9] J. C. Zegers, E. Semsar-Kazerooni, J. Ploeg, N. van de Wouw, and H. Nijmeijer, "Consensus-based Bi-directional CACC for Vehicular Platooning," in *American Control Conference (ACC 2016)*. Boston, MA: IEEE, Jul. 2016, pp. 2578–2584.

[10] S. Santini, A. Salvi, A. S. Valente, A. Pescapè, M. Segata, and R. Lo Cigno, "A Consensus-based Approach for Platooning with Inter-Vehicular Communications and its Validation in Realistic Scenarios," *IEEE Transactions on Vehicular Technology*, vol. 66, no. 3, pp. 1985–1999, Mar. 2017.

[11] S. Oncu, J. Ploeg, N. Van De Wouw, and H. Nijmeijer, "Cooperative Adaptive Cruise Control: Network-Aware Analysis of String Stability," *IEEE Transactions on Intelligent Transportation Systems*, vol. 15, no. 4, pp. 1527–1537, Aug. 2014.

[12] C. Lei, E. van Eenennaam, W. Wolterink, G. Karagiannis, G. Heijenk, and J. Ploeg, "Impact of Packet Loss on CACC String Stability Performance," in *11th International Conference on ITS Telecommunications (ITST 2011)*, Saint Petersburg, Russia, Aug. 2011, pp. 381–386.

[13] M. Segata, B. Bloessl, S. Joerer, C. Sommer, M. Gerla, R. Lo Cigno, and F. Dressler, "Towards Communication Strategies for Platooning: Simulative and Experimental Evaluation," *IEEE Transactions on Vehicular Technology*, vol. 64, no. 12, pp. 5411–5423, Dec. 2015.

[14] P. Fernandes and U. Nunes, "Platooning With IVC-Enabled Autonomous Vehicles: Strategies to Mitigate Communication Delays, Improve Safety and Traffic Flow," *IEEE Transactions on Intelligent Transportation Systems*, vol. 13, no. 1, pp. 91–106, Mar. 2012.

[15] L.-N. Hoang, E. Uhlemann, and M. Jonsson, "An Efficient Message Dissemination Technique in Platooning Applications," *IEEE Communications Letters*, vol. 19, no. 6, pp. 1017–1020, March 2015.

[16] A. Böhm and K. Kunert, "Data age based MAC scheme for fast and reliable communication within and between platoons of vehicles," in *12th IEEE International Conference on Wireless and Mobile Computing, Networking and Communications (WiMob 2016)*. New York, NY: IEEE, October 2016, pp. 1–9.

[17] A. Böhm, M. Jonsson, K. Kunert, and A. Vinel, "Context-Aware Retransmission Scheme for Increased Reliability in Platooning Applications," in *6th IFIP/IEEE International Workshop on Communication Technologies for Vehicles (Nets4Cars 2014-Spring)*. Offenburg, Germany: Springer, May 2014, pp. 30–42.

[18] A. Balador, A. Böhm, E. Uhlemann, C. T. Calafate, and J.-C. Cano, "A Reliable Token-Based MAC Protocol for Delay Sensitive Platooning Applications," in *82nd IEEE Vehicular Technology Conference (VTC2015-Fall)*. Boston, MA: IEEE, September 2015.

[19] M. Segata, F. Dressler, and R. Lo Cigno, "Jerk Beaconing: A Dynamic Approach to Platooning," in *7th IEEE Vehicular Networking Conference (VNC 2015)*. Kyoto, Japan: IEEE, December 2015, pp. 135–142.

[20] J. Ploeg, E. Semsar-Kazerooni, G. Lijster, N. van de Wouw, and H. Nijmeijer, "Graceful Degradation of CACC Performance Subject to Unreliable Wireless Communication," in *16th International IEEE Conference on Intelligent Transportation Systems (ITSC 2013)*. The Hague, The Netherlands: IEEE, October 2013, pp. 1210–1216.

[21] M. Abualhoul, M. Marouf, O. Shagdar, and N. Fawzi, "Platooning Control Using Visible Light Communications: A Feasibility Study," in *IEEE Intelligent Transportation Systems Conference (ITSC 2013)*. The Hague, The Netherlands: IEEE, Oct. 2013.

[22] M. Segata, R. Lo Cigno, H.-M. Tsai, and F. Dressler, "On Platooning Control using IEEE 802.11p in Conjunction with Visible Light Communications," in *12th IEEE/IFIP Conference on Wireless On demand Network Systems and Services (WONS 2016)*. Cortina d'Ampezzo, Italy: IEEE, January 2016, pp. 124–127.

[23] P. Fernandes and U. Nunes, "Platooning with DSRC-based IVC-enabled Autonomous Vehicles: Adding Infrared Communications for IVC Reliability Improvement," in *IEEE Intelligent Vehicles Symposium (IV 2012)*. Alcala de Henares, Spain: IEEE, June 2012, pp. 517–522.

[24] M. Y. Abualhoul, M. Marouf, O. Shag, and F. Nashashibi, "Enhancing the Field of View Limitation of Visible Light Communication-based Platoon," in *6th IEEE International Symposium on Wireless Vehicular Communications (WiVec 2014)*. Vancouver, BC: IEEE, September 2014, pp. 1–5.

[25] S. Ishihara, R. V. Rabsatt, and M. Gerla, "Improving Reliability of Platooning Control Messages Using Radio and Visible Light Hybrid Communication," in *7th IEEE Vehicular Networking Conference (VNC 2015)*. Kyoto, Japan: IEEE, December 2015, pp. 96–103.

[26] C. Campolo, A. Molinaro, G. Araniti, and A. Berthet, "Better Platooning Control Toward Autonomous Driving: An LTE Device-to-Device Communications Strategy That Meets Ultralow Latency Requirements," *IEEE Vehicular Technology Magazine*, vol. 12, no. 1, pp. 30–38, March 2017.

[27] G. Giordano, "Structural Analysis and Control of Dynamical Networks," Ph.D. dissertation, Università degli Studi di Udine, 2016.

[28] S. Jayasuriya and M. Franchek, "A Class of Transfer Functions with Non-negative Impulse Response," *Journal of dynamic systems, measurement, and control*, vol. 113, no. 2, pp. 313–315, Jun. 1991.

[29] Y. Liu and P. H. Bauer, "Sufficient Conditions for Non-negative Impulse Response of Arbitrary-order Systems," in *IEEE Asia Pacific Conference on Circuits and Systems (APCCAS 2008)*. Macao, China: IEEE, Dec. 2008, pp. 1410–1413.

[30] M. Segata, S. Joerer, B. Bloessl, C. Sommer, F. Dressler, and R. Lo Cigno, "PLEXE: A Platooning Extension for Veins," in *6th IEEE Vehicular Networking Conference (VNC 2014)*. Paderborn, Germany: IEEE, Dec. 2014, pp. 53–60.

[31] M. Segata and R. Lo Cigno, "Automatic Emergency Braking - Realistic Analysis of Car Dynamics and Network Performance," *IEEE Transactions on Vehicular Technology*, vol. 62, no. 9, pp. 4150–4161, Oct. 2013.

[32] P. Greibe, "Braking distance, friction and behavior," Trafitec, Scion-DTU, Technical Report, Jul. 2007.